CHIN. PHYS. LETT. Vol. 34, No. 11 (2017) 114203

Active Anomalous Transmission and Its Application in Compensating Waveform Distortions *

Chun Wang(王春)[1], Lei Chen(陈雷)[2], Shan Qiao(乔闪)[3], Yu-Zhou Shen(沈昱舟)[1], An-Jie Zhu(朱安杰)[1], De-Xin Ye(叶德信)[1], Chang-Zhi Li(李长志)[4], Li-Xin Ran(冉立新)[1]**

[1]*Laboratory of Applied Research on Electromagnetics, Zhejiang University, Hangzhou 310027*
[2]*Beijing Electro-mechanical Engineering Institute, Beijing 100074*
[3]*Zhejiang University City College, Hangzhou 310015*
[4]*Department of Electrical and Computer Engineering, Texas Tech University, TX 79409, USA*

(Received 17 July 2017)

In theory, engineered anomalous transmission in passive materials and waveguide devices can be used to compensate for waveform distortions. However, they suffer from inherent dissipation. Recently, active non-Foster elements with imaginary immittance monotonically decreasing with frequency have shown important potentials in broadening bandwidths of electromagnetic devices. So far, they are implemented based on negative impedance convertors (NICs) loaded with Foster devices. This makes them intrinsically one-port elements and thus cannot be used to compensate for distortions of signals. We construct a two-port network with a non-Foster transmission coefficient based on an unconventional use of NICs. Simulation and experiments show that it can compensate for extremely distorted signals. The proposed method can be used to broaden existing applications in different areas such as antennas, circuits and systems, and physical-layer signal processing.

PACS: 42.65.Re, 02.60.Cb DOI: 10.1088/0256-307X/34/11/114203

For signals transmitting through materials, waveguides and circuits, waveform distortions are inevitable due to various frequency dispersions. Consequently, the signal distortion is one of the major limiting factors in electronic systems. So far, it has been well recognized that engineered anomalous transmission in passive materials and waveguide devices can be used to compensate for waveform distortions in physical layers.[1–3] However, they suffer from severe, inherent dissipations in anomalous dispersion bands.

Recently, non-Foster elements (NEs) with their imaginary immittance decreasing with frequency have attracted many interests.[4–6] Theoretical analyses and experimental demonstrations showed that such active elements can exhibit 'negative' reactance.[7] This special characteristic can be used to broaden the bandwidth of radio frequency (RF) devices such as electrically small antennas[8,9] and metamaterials,[10] implying a wide range of potential applications. So far, NEs were implemented based on negative impedance convertors (NICs) loaded with Foster devices. This makes them intrinsically one-port elements that only have reflection coefficients. Consequently, they were mainly used to compensate for parallel reactance of target devices. This limits the use of conventional NEs for applications such as the compensation for waveform distortion of signals.

In this work, we construct a two-port non-Foster network with an unconventional use of a floating NIC based on an operational amplifier (OP AMP). Compared with conventional one-port NEs, this network can be connected in series in circuits. With a non-Foster transmission coefficient, it can also be used to compensate for waveform distortion of signals. Theoretical analysis, simulation and experimental results verified the effectiveness of the proposed network. Being an active network, it can possess a compact size and tunable anomalous frequency responses, exhibiting a unique advantage compared with the existing passive solutions.

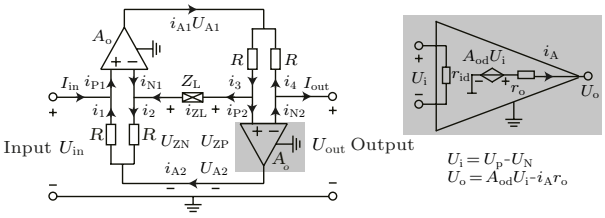

Fig. 1. Circuit analysis for the proposed two-port network.

Figure 1 shows the circuit topology of a floating NIC based on dual OP AMPs, whose equivalent circuit is shown in the greyed inset. As discussed in Ref. [11], when I_{in} and I_{out} are considered as the differential input currents and Z_L as the load impedance, the input differential impedance can be calculated as $-Z_L$. In the following we will prove that if I_{in} and I_{out} shown in Fig. 1 can be considered as two single-ended input and output currents, the floating NIC can be converted into a two-port network with a non-Foster transmission coefficient.

With the notations in Fig. 1 and applying the Kirchhoff laws, the $ABCD$ matrix can be obtained

*Supported by the National Natural Science Foundation of China under Grant Nos 61771421, 61771422, 61528014 and 6140139, and the Zhejiang Provincial Natural Science Foundation under Grant No LY16F010009.
**Corresponding author. Email: ranlx@zju.edu.cn
© 2017 Chinese Physical Society and IOP Publishing Ltd

from the circuit equations

$$MU_{\rm in} = \Big(\frac{1}{r_{\rm id}} + \frac{1}{2R} - \frac{1}{2R+4r_{\rm o}}\Big)U_{\rm ZN} + I_{\rm in} + \frac{A_{\rm o}}{R+2r_{\rm o}}U_{\rm ZP} - \frac{A_{\rm o}}{R+2r_{\rm o}}U_{\rm out}, \quad (1)$$

$$-MU_{\rm out} = -\Big(\frac{1}{r_{\rm id}} + \frac{1}{2R} - \frac{1}{2R+4r_{\rm o}}\Big)U_{\rm ZP} + I_{\rm out} + \frac{A_{\rm o}}{R+2r_{\rm o}}U_{\rm ZN} - \frac{A_{\rm o}}{R+2r_{\rm o}}U_{\rm in}, \quad (2)$$

$$U_{\rm ZN} = -[N + Z_{\rm L}(R+2r_{\rm o})(2A_{\rm o}I_{\rm out} - I_{\rm in}) + Z_{\rm L}(1-4A_{\rm o}^2)U_{\rm in} + 4A_{\rm o}Z_{\rm L}U_{\rm out}] /[2R + Z_{\rm L} + 4r_{\rm o} + 4A_{\rm o}^2 Z_{\rm L}], \quad (3)$$

$$U_{\rm ZP} = -[N + Z_{\rm L}(R+2r_{\rm o})(I_{\rm out} - 2A_{\rm o}I_{\rm in}) + Z_{\rm L}(1-4A_{\rm o}^2)U_{\rm out} - 4A_{\rm o}Z_{\rm L}U_{\rm in}] /[2R + Z_{\rm L} + 4r_{\rm o} + 4A_{\rm o}^2 Z_{\rm L}], \quad (4)$$

$$M = \frac{1}{r_{\rm id}} + \frac{1}{2R} + \frac{1}{2R+4r_{\rm o}}, \quad (5)$$

$$N = (R+2r_{\rm o})(U_{\rm out} + U_{\rm in}) + 2A_{\rm o}(R+2r_{\rm o})(U_{\rm out} - U_{\rm in}) + (R+2r_{\rm o})^2(I_{\rm out} - I_{\rm in}). \quad (6)$$

When the open loop differential gain of the OP AMPs is sufficiently large, the transmission coefficient $B = U_{\rm in}/I_{\rm out}$ can be simplified to

$$B = -\Big[9Z_{\rm L}^2(1+2R) + \Big(\frac{2R+Z_{\rm L}}{A_{\rm o}}\Big)^2 + 4A_{\rm o}Z_{\rm L}(3A_{\rm o}Z_{\rm L} - R)\Big] \Big/ \Big\{2R\Big(1 - \frac{2}{A_{\rm o}}\Big) + Z_{\rm L}\Big[12A_{\rm o}\Big(A_{\rm o} - \frac{Z_{\rm L}}{R} - \frac{5}{3}\Big) + \Big(1 - \frac{Z_{\rm L}}{A_{\rm o}R} - \frac{4}{A_{\rm o}}\Big)\Big]\Big\}. \quad (7)$$

Although B is no longer directly proportional to $-Z_{\rm L}$ as the original floating NIC, both its real (resistive) and imaginary (reactive) parts can exhibit series non-Foster responses.

Figure 2 shows the reactive response of B. All the curves were calculated by Eq. (7) when the output port is open circuit. In Fig. 2(a), $Z_{\rm L}$ is set as a fixed 10-pF capacitor, and the resistance of the bias resistor R is changed from 3 to 40 Ω. In Fig. 2(b), A_0 is set as 170, R is set as 100 Ω, and $Z_{\rm L}$ is set as a capacitor, whose capacitance changes from 3 to 40 pF. Note that according to Ref. [12], $Z_{\rm L}$ cannot be inductive, otherwise a self-excited oscillation would be induced. It is seen that both reactive responses of B are non-Foster in a wide bandwidth, and such non-Foster responses can be continuously changed by tuning R and $Z_{\rm L}$, respectively.

Next, we perform circuit simulations to verify the above theoretical analysis based on a commercial circuit simulator, Multism™ (http://www.ni.com/multisim). The simulation model is shown in Fig. 3(a), where the circuit structure is the same as that in Fig. 1. In the model, the integrated dual RF OP AMP, Texas Instruments OPA2695, was chosen, and the vendor-provided SPICE model was used in the simulation. The simulation frequency was swept from 1 to 100 MHz, and the built-in software vector network analyzer (VNA) was used to measure the transmission coefficient B.

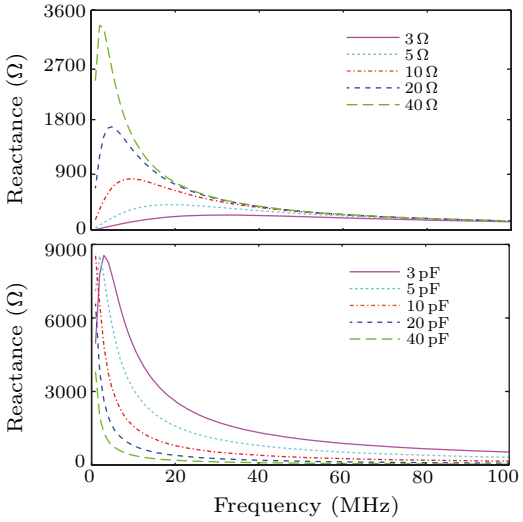

Fig. 2. Series non-Foster response due to the transmission coefficient B. (a) Reactive response with respect to a changing R. (b) Reactive response with respect to a changing capacitive $Z_{\rm L}$.

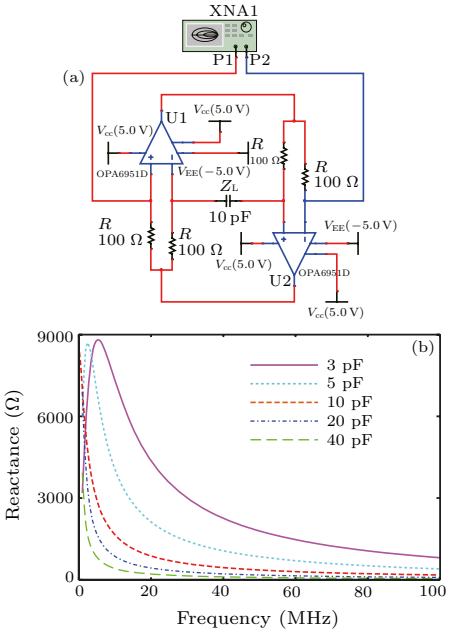

Fig. 3. Circuit simulation based on given SPICE parameters. (a) Circuit simulation model. (b) Simulated reactive response of the transmission coefficient.

In the simulation, the OPA2695 was biased by direct current (DC) voltages of +/−5 V, and R was set as 100 Ω. To compare with the analytical results, $Z_{\rm L}$ was set as a capacitor, whose capacitance was also increased from 3 to 40 pF. The simulated results are

shown in Fig. 3(b). It is seen that the non-Foster reactive responses of the transmission coefficient are close to those calculated by Eq. (7), verifying the effectiveness of the circuit analysis.

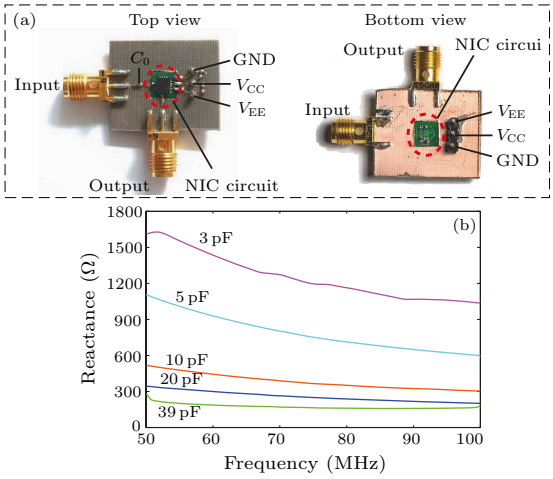

Fig. 4. Experimental verification of the non-Foster coefficient. (a) Hardware implementation of the two-port non-Foster network. The size of the non-Foster elements (the small green boards) is $5\times5\,\mathrm{mm}^2$. (b) Experimental results of the non-Foster transmission coefficient.

To experimentally verify the above analysis, the proposed network was physically implemented, as shown in Fig. 4(a). In the implementation, the OPA2695 was chosen as the key component, and two coaxial RF connectors were used as the input and output ports. The power supplies of the OP AMPs were $+/-5$ V. The resistance of R was 100 Ω and the capacitance of Z_{L} was changed from 3 to 39 pF. According to Ref. [12], to ensure the stability of the NIC, a series capacitor C_0 was added before the NIC, thus the total reactance remains positive.

To obtain the non-Foster transmission coefficient, a VNA, Agilent 8722ES, was used to measure S. Limited by the lower-end frequency of this VNA, the measured frequency was between 50 and 100 MHz. The reactive transmission response can be retrieved from the measured S parameters according to the conversion between S matrix and $ABCD$ matrix. Figure 4(b) plots retrieved responses for different capacitive loads. It can be seen that the experimental negative slopes comply with the simulated results in Fig. 3(b).

To experimentally verify the waveform compensation effect, an extremely distorted signal was used. A 37.5-MHz square-wave signal was generated first, and then filtered by a high-pass filter consisting of a 100-Ω shunt resistor and a 100-pF series capacitor. Since the high-pass filter's cutoff frequency is 100 MHz, the primary component and the second order harmonic of the square-wave signal would be significantly attenuated. Finally, this extremely distorted signal was fed into the NIC circuit. To maintain the balance of the NIC, the output port was loaded with the same resistance and capacitance as those of the input port. In the measurement, the resistance R was fixed at 100 Ω, and the capacitive Z_{L} was tuned to 180 pF to obtain the optimal compensation.

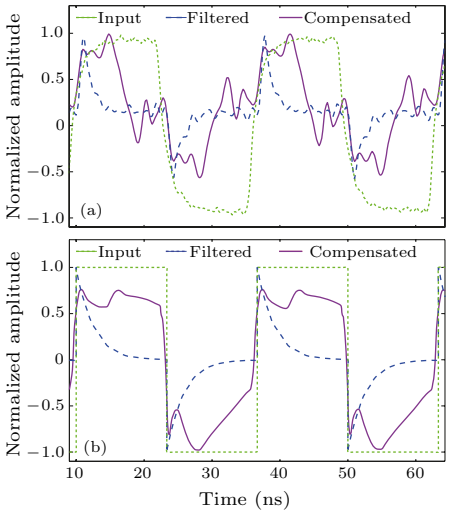

Fig. 5. Experimental compensation for an extremely distorted waveform. (a) Experimental results. (b) Simulated results under the same conditions.

Figure 5(a) shows the original (in green), distorted (in blue) and compensated (in purple) waveforms captured by an oscilloscope. For comparison, Fig. 5(b) shows the results simulated under the same conditions. It is seen that after filtering, the waveforms are extremely distorted and attenuated as expected. After compensation, however, the severely distorted waveforms are effectively corrected. The imaginary part of Z_{21} simulated in achieving Fig. 5(b) is $j0.084$, corresponding to a 0.36-nH inductance in the operating bandwidth centered at 37.5 MHz. It implies that the 100-pF capacitance in the high-pass filter has been slightly over-compensated into a weak inductance, which is the essential mechanism behind this compensation. Since the high-order harmonics of the original signal are much higher than 100 MHz, the OP AMP-based NIC is unable to compensate for all the harmonics. Although the extremely distorted waveform is not fully corrected, the compensation effect can be clearly observed.

In conclusion, we have proposed a non-Foster network based on a floating NIC. Different from conventional NEs, this network can be connected in series in circuits, exhibiting a non-Foster transmission coefficient that can potentially compensate for waveform distortions due to Foster frequency dispersions. Simulation and experiments show that it can be used to compensate for extremely distorted signals. Being an active network, it can possess a compact size and tuneable anomalous frequency responses, exhibiting a unique advantage compared with existing passive solutions. If wideband OP AMPs such as Texas Instrument LMH5401, whose operating bandwidth can reach 8 GHz, can be used, the proposed NEs would be able to work at GHz frequencies. The proposed approach can broaden the conventional applications in

different areas such as coding metamaterials,[13] antennas, circuits and systems, and physical-layer signal processing.

References

[1] Wang C, Zhu Z B, Cao C, Qiao S, Li C Z and Ye D X 2017 *AIP Adv.* **7** 045208
[2] Li Y H, Fan W D and Sheng Q Q 2010 *Chin. Phys. Lett.* **27** 114211
[3] Chen X W, Jiang Y L, Leng Y X, Liu J, Ge X C, Li R X and Xu Z Z 2006 *Chin. Phys. Lett.* **23** 1198
[4] Mirzaei H and Eleftheriades G V 2013 *IEEE Trans. Microwave Theory Tech.* **61** 4322
[5] Debogovic T, Hrabar S and Perruisseau-Carrier J 2013 *Electron. Lett.* **49** 239
[6] Long J, Jacob M and Sievenpiper D F 2014 *IEEE Trans. Microwave Theory Tech.* **62** 789
[7] Foster R M 1924 *Bell Syst. Tech. J.* **3** 259
[8] Yoon I J, Christensen S, Zhurbenko V, Kim O S and Breinbjerg O 2016 *Electron. Lett.* **52** 996
[9] Zhu N and Ziolkowski R W 2011 *IEEE Antennas Wireless Propag. Lett.* **10** 1582
[10] Gao F, Zhang F, Long J, Jacob M and Sievenpiper D 2014 *Electron. Lett.* **50** 1616
[11] Antoniou A 1972 *IEEE Trans. Circuit Theory* **19** 209
[12] Ugarte-Munoz E, Hrabar S, Segovia-Vargas D and Kiricenko A 2012 *IEEE Trans. Antennas Propag.* **60** 3490
[13] Cui T J, Qi M Q, Wan X, Zhao J and Cheng Q 2014 *Light: Sci. Appl.* **3** e218